Cancer Chemotherapy and Pharmacology (2019) 84:729–738
https://doi.org/10.1007/s00280-019-03903-5

ORIGINAL ARTICLE

Species-specific optimization of PEG~SN-38 prodrug pharmacokinetics and antitumor effects in a triple-negative BRCA1-deficient xenograft

Shaun D. Fontaine[1] · Byron Hann[2] · Ralph Reid[1] · Gary W. Ashley[1] · Daniel. V. Santi[1]

Received: 27 February 2019 / Accepted: 4 July 2019 / Published online: 18 July 2019

Abstract

Purpose Optimal efficacy of a macromolecular prodrug requires balancing the rate of drug release with the rate of prodrug elimination. Since circulating macromolecules have different elimination rates in different species, a prodrug optimal for one species will likely not be for another. The objectives of this work were (a) to develop an approach to optimize pharmacokinetics of a PEG~SN-38 prodrug in a particular species, (b) to use the approach to predict the pharmacokinetics of various prodrugs of SN-38 in the mouse and human, and (c) to develop a PEG~SN-38 conjugate that is optimized for mouse tumor models.

Methods We developed models that describe the pharmacokinetics of a drug released from a prodrug by the relationship between the rates of drug release and elimination of the prodrug. We tested the model by varying the release rate of SN-38 from PEG~SN-38 conjugates in the setting of a constant prodrug elimination rate in the mouse. Finally, we tested the antitumor efficacy of a PEG~SN-38 optimized for the mouse.

Results Optimization of a PEG~SN-38 prodrug was achieved by adjusting the rate of SN-38 release such that the ratio of $t_{1/2,\beta}$ of released SN-38 to the $t_{1/2}$ of prodrug elimination was 0.2–0.8. Using this approach, we could rationalize the efficacy of previous PEGylated SN-38 prodrugs in the mouse and human. Finally, a mouse-optimized PEG~SN-38 showed remarkable antitumor activity in BRCA1-deficient MX-1 xenografts; a single dose gave tumor regression, suppression, and shrinkage of massive tumors.

Conclusions The efficacy of a macromolecular prodrug can be optimized for a given species by balancing the rate of drug release from the carrier with the rate of prodrug elimination.

Keywords Drug delivery · Top1 · Half-life extension · PEGylated prodrugs

Introduction

CPT-11 (Irinotecan) is a mainstay of cancer chemotherapy. It serves as a water-soluble prodrug for SN-38, which stabilizes the topoisomerase I (Top1)-DNA complex and inhibits the enzyme. As a mechanism-based DNA damaging agent, the drug has taken on added importance in enhancing DNA damage response defects in tumors.

Inhibition of Top1 by SN-38 leads to DNA strand breaks that, if unrepaired, lead to cell death. However, CPT-11 is a less than ideal prodrug and has notoriously complex pharmacokinetics and metabolism [1, 2]. In the liver, CPT-11 is partly inactivated by CYP3A and partly converted to SN-38 by carboxyesterase 2; SN-38 is then metabolized by hepatic UGT1A to its 10-glucuronide, SN-38G, which is transported to bile. After biliary excretion, intestinal bacterial β-glucuronidase causes its reconversion to SN-38, which can result in severe GI toxicity. These multiple metabolic and transport processes lead to high interpatient variability of CPT-11 pharmacokinetics, efficacy, and toxicity. Certainly,

Electronic supplementary material The online version of this article (https://doi.org/10.1007/s00280-019-03903-5) contains supplementary material, which is available to authorized users.

✉ Daniel. V. Santi
daniel.v.santi@prolynxllc.com

[1] ProLynx, 455 Mission Bay Boulevard South, Suite 341, San Francisco, CA 94158, USA

[2] University of California San Francisco, 1450 3rd Street, San Francisco, CA 94158, USA

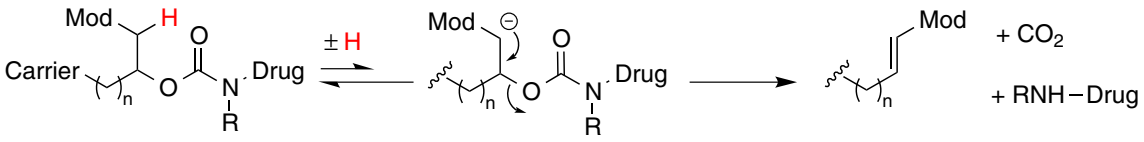

Scheme 1 Generic mechanism of drug release from PEGylated conjugates

a more efficient and effective prodrug of SN-38 would be desirable.

A slow-releasing macromolecular prodrug of SN-38 should provide significant advantages over CPT-11 [3]. First, direct release of SN-38 would avert the hepatic metabolism required for CPT-11, and may reduce toxic GI effects. Second, without dose-limiting GI toxicity, higher doses of the drug should be tolerable and provide higher tumor exposure. Third, protracted release of SN-38 would show longer systemic exposure with a lower C_{max}. This could reduce toxicities seen with CPT-11, ensure that drug–Top1–DNA complexes persist long enough to be converted to DNA damage, and increase the likelihood that cells pass through the Top1-sensitive S-phase during the exposure period. Finally, the macromolecular component of the prodrug may cause tumor accumulation via the enhanced permeability and retention effect [4] and increases exposure to counteract effects of drug efflux [5].

Several long-acting esterase-cleavable PEGylated prodrugs of SN-38 or CPT-11 have been investigated in preclinical and clinical studies [6–11]. In mouse models, the ester-linked prodrugs provide a longer half-life and higher SN-38 exposure than does CPT-11, accumulate in tumors and show high antitumor efficacy. However, efficacy in the mouse has not translated well to the human, and none have successfully achieved regulatory approval. Below, we posit that the release rates of such esterase-cleavable prodrugs are suitable for use in the mouse, but too fast for optimal efficacy in the human.

To optimize the efficacy of such macromolecular prodrugs, the rate of drug release must be balanced with the rate of renal elimination. Although the cleavage rate of a linker may or may not be species dependent, circulating PEG conjugates have different renal elimination rates in different species; for example, the elimination half-life of a 4-arm PEG_{40kDa} is ~ 1 day in the mouse, ~ 2 days in the rat, and ~ 7 days in the human [12]. Thus, a given PEG~SN-38 will have different prodrug pharmacokinetics in each species, and a conjugate that is optimal for one will likely not be for another.

We have developed a general approach for half-life extension of therapeutics in which a drug is covalently tethered to a long-lived carrier by a linker that slowly cleaves by β-elimination to release the drug (Scheme 1) [12, 13]. The cleavage rate is controlled by the nature of an electron-withdrawing "modulator" (Mod) that attenuates the acidity of the adjacent C–H bond, and is unaffected by enzymes or general acid/base catalysts.

The carrier used for β-eliminative linkers can be a long-lived circulating macromolecule—such as high molecular weight PEG [12]. The prodrug is usually eliminated with a half-life similar to the carrier, and the longest achievable elimination half-life of the released drug is limited by the renal elimination rate of the prodrug.

We adapted β-eliminative carbamate linkers for use with phenols [14] and produced PEG_{40kDa}~SN-38 prodrugs with a range of drug release rates [3]. The PEG_{40kDa}~SN-38 conjugates **1A–C** (Scheme 2) release SN-38 with in vivo cleavage half-lives as short as 12 h (**1A**) to as long as 360 h (**1C**) [3]. The longest-lived conjugate with a -CN modulator (**1C**; X = –CONH–)—designated as PLX038—has entered Phase 1 clinical trials (NCT02646852; https://clinicaltrials.gov/). To date, very long-acting PLX038 has been studied in the rat or larger species. Studies in the mouse—the most common host for human tumor models—have not been undertaken because the rapid renal elimination of the slow-cleaving PLX038 prodrug in this species limits exposure to free SN-38.

In the present work, we describe an approach for optimizing PEG_{40kDa}~SN-38 as a prodrug in a particular species, and analyze the pharmacokinetic suitability of long-acting PEGylated prodrugs of Top1 inhibitors in the mouse and in the human. Using this approach, we developed a PEG_{40kDa}~SN-38—designated as PLX038A—that has optimal pharmacokinetics

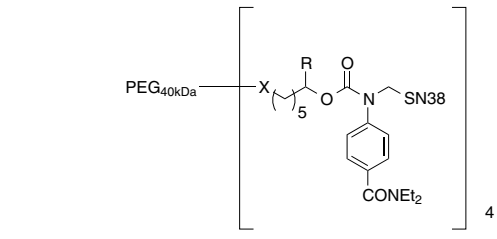

Scheme 2 Structures of the evaluated PEG~SN-38 conjugates

for use in mouse tumor models. Finally, we demonstrate the remarkable antitumor effects of PLX038A in the triple negative breast cancer BRCA1-deficient human xenograft MX-1.

Methods

Detailed descriptions of materials and procedures used for syntheses, pharmacokinetic studies, and tumor xenograft experiments are presented in the Supplementary Information (SI).

Synthesis

PEG~SN-38 conjugates were prepared as previously described [3] with modifications provided in SI.II.

Pharmacokinetics

Serial micro-sampling pharmacokinetic assays in mice were performed by Charles River using male CD-1 mice ~ 25 g in weight. Dosing solutions of PEG~SN-38 contained ≤ 8 mM SN-38 in isotonic 10 mM NaOAc, pH 5.0. Injections were performed i.p. to deliver from 3.6 to 120 µmol/kg. Serial blood samples were collected from each animal via tail snip and plasma was prepared and stored at − 80 °C until HPLC analysis; C18 HPLC was performed using a gradient of H_2O and MeCN containing 0.1% TFA. Pharmacokinetic modeling used equations described in the text and data analyses and plotting were performed using Prism 8.0. Statistics used are presented with the data reported in the text and SI. Details are provided in SI.III.

Animal tumor model

Animal studies were carried out in accordance with UCSF Institutional Animal Care and Use Committee. Tumor xenografts were established by subcutaneous implants of MX-1 tumor fragments into the right flank of female NCr nude mice. When tumors reached ~ 100–200 mm^3, dosing solutions of PLX038A were administered i.p. to deliver 4 to 120 µmol SN-38/kg, and tumor volumes were determined by caliper measurement vs. time. The nomenclature used for describing tumor growth in individual mice was as proposed by Houghton et al. [15]. Details are provided in SI.IV.

Results

Pharmacokinetic modeling

Scheme 3 depicts the one-compartment model that describes the pharmacokinetics of releasable PEG~SN-38 conjugates injected i.v. [12], and the two-compartment model after i.p. injection. Here, k_1 is the rate constant for cleavage of the linker, k_2 is the rate of elimination of the free drug, and k_3 is the rate of elimination of the conjugate. For i.p. injection, there also is an absorption rate, k_a, for the conjugate transfer from the i.p. to central compartments.

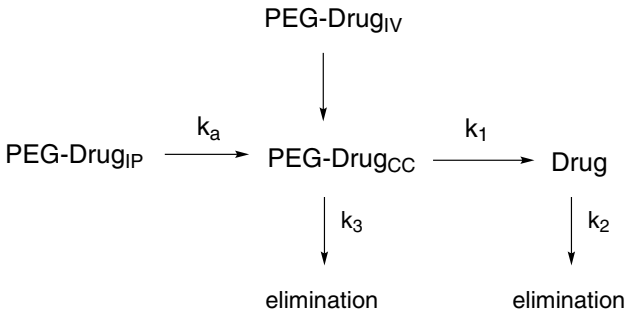

Scheme 3 Pharmacokinetic model for releasable PEG~SN-38 after i.v. or i.p injection

After i.p. injection, the PEG conjugate and the released drug in the central compartment (CC) are described by Eqs. 1 and 2 [12] (see SI).

$$[\text{PEG}-\text{Drug}]_{CC} = [\text{PEG}-\text{Drug}]_0 \times e^{-(k_1+k_3)t}, \quad (1)$$

$$[\text{Drug}]_{CC} = [\text{PEG–Drug}]_0 \times (V_{d,conj}/V_{d,drug}) \times \left(k_1/k_2\right) \times e^{-(k_1+k_3)t}. \quad (2)$$

After absorption of PEG~SN-38, the slopes of plots of ln[PEG-Drug]$_{CC}$ and ln[Drug]$_{CC}$ vs. time are parallel and apparent elimination rates, k_β, of both prodrug and released drug are described by Eq. 3.

$$k_{\beta,\text{PEG~SN-38}} = k_{\beta,\text{SN-38}} = k_1 + k_3. \quad (3)$$

Hence, the $t_{1/2,\beta}$ of the released SN-38 is determined by the cleavage rate of the linker (k_1) and elimination rate of the conjugate (k_3).

I.p. vs. i.v. injection of PEG~SN-38

We determined the suitability of administering PEG_{40kDa}~SN-38 by i.p. vs. the more common i.v. injections used for such conjugates. The same amounts of the stable PEG_{40kDa}~SN-38 conjugate **1D** (Scheme 2) were injected in mice by i.v. or i.p. routes, and **1D** in plasma samples was measured over time (Fig. 1a). The $t_{1/2,\beta}$ of the PEG~SN-38 administered by either route is ~ 20 h. The identical AUC_{64hr} values for PEG~SN-38 by i.v. and i.p. routes indicate an i.p. bioavailability of ~ 96%. The $V_{d,ss}$ of **1D** of 0.08 L/kg (Table S1) is similar to the vascular volume of the mouse so once absorbed the conjugate is confined to the

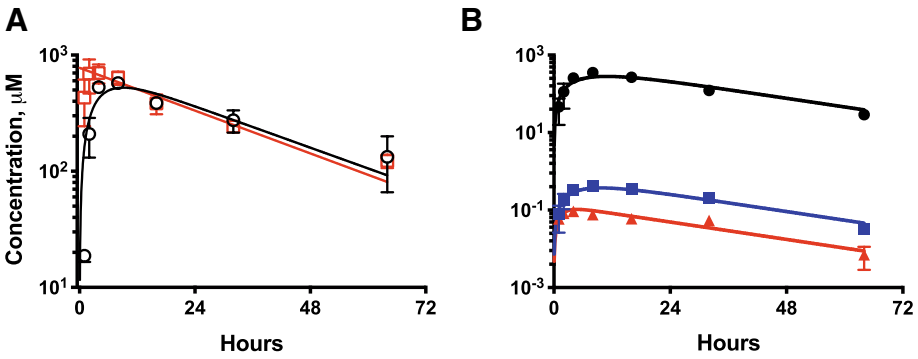

Fig. 1 *C* vs. *t* plots of PEG~SN-38 conjugates in the mouse. **a** i.p. (black unfilled circle) vs. i.v. (red unfilled square) dosing of stable PEG~SN-38 1D; k_β and AUC_{64h} values were 0.036 ± 0.005/h and 19.5 ± 0.90 mM*h, respectively, for i.v. injection and 0.034 ± 0.019/h and 18.7 ± 1.5 mM*h, respectively, for i.p. **b** *C* vs. *t* curves of **1B** (black filled circle), SN-38 (blue filled square), and SN-38G (red filled upward triangle) after i.p. injection of 40 μmol/kg **1B**. Data show the average ± SEM and lines are least squares best fits to Eq. 1 weighted by $1/SD^2$

Table 1 Pharmacokinetic parameters for PEG~SN-38 conjugates in the mouse and human

Cmpd, Mod	$t_{1/2,\beta}$ (h)[a]	$t_{1/2,3}$ (h)[b]	$t_{1/2,1}$ (h)[c]	$t_{1/2,1}/t_{1/2,3}$	$t_{1/2,\beta}/t_{1/2,3}$	$k_1/(k_1+k_3)$ [AUC_{rel}]	$C^d_{max,rel}$
Mouse							
1D, None	22	22	NA	NA	1	NA	
1A, $–SO_2Ph$	9	22	13	0.59	0.41	0.63	6.0
1B, $–SO_2Me$	17	22	75	3.4	0.77	0.23	1
1C, –CN	21[c]	22	360[e]	16	0.94	0.06	0.21
Enz-2208	12[f]	22	25[3]	1.14	0.53	0.47	3.0
Human							
1C, –CN	115	168 [g]	360[d]	2.1	0.68	0.32	1

[a]Experimentally determined

[b]Determined by stable surrogate **1D**

[c]Calculated from Eq. 3

[d]$C_{max,rel}$ in mouse is normalized to the C_{max} of **1B**, and in humans, to the predicted C_{max} of **1C**, using Eqs. 5 and 7

[e]From [3]

[f]From Fig. 5 in [16]

[g]A $t_{1/2,3}$ of 168 h was estimated using $t_{1/2,1}$ of 360 h [3] and $t_{1/2,\beta}$ = 115 h

[h]From Table 4 in [17]

vascular compartment. Figure 1b shows *C* vs. *t* plots of the PEG~SN-38 **1B** along with free SN-38 and SN-38G after a single i.p. injection of 40 μmol/kg PLX038A (described below).[1]

Prodrug optimization

Optimizing a prodrug for a particular species requires balancing the linker cleavage rate with the rate of prodrug renal elimination. First, we assess values for $t_{1/2,\beta}$, $t_{1/2,1}$, and $t_{1/2,3}$. Here, $t_{1/2,\beta}$ is determined experimentally and $t_{1/2,3}$ is estimated with a stable surrogate of the prodrug, such as **1D**. Then $t_{1/2,1}$ is calculated using Eq. 3, and the ratios $t_{1/2,1}/t_{1/2,3}$, $t_{1/2,\beta}/t_{1/2,3}$, and $k_1/(k_1+k_3)$ are determined (Table 1).

Since the $t_{1/2,\beta}$ of a released drug is limited by the $t_{1/2,3}$ of the prodrug, the fraction of the maximum achievable half-life extension ($F_{t_{1/2,max}}$) can be quantified as $t_{1/2,\beta}/t_{1/2,3}$. This parameter can be related to the drug cleavage rate, k_1, by a plot of $t_{1/2,\beta}/t_{1/2,3}$ vs. $t_{1/2,1}/t_{1/2,3}$ (Fig. 2). Also, the $t_{1/2,1}/t_{1/2,3}$ is inversely related to the efficiency of drug utilization—the fraction of prodrug converted to the drug—described by $k_1/(k_1+k_3)$ [3].

[1] Doses of PEG~SN-38 refer to the amount of conjugated SN-38 delivered.

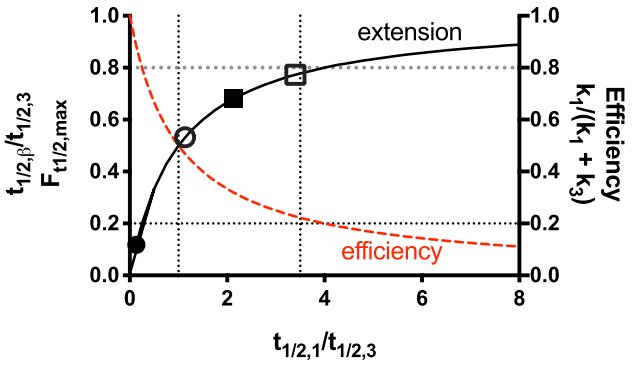

Fig. 2 Plot of $t_{1/2,\beta}/t_{1/2,3}$ vs. $t_{1/2,1}/t_{1/2,3}$ and efficiency $(k_1/(k_1+k_3))$ of PEG~SN-38 conjugates. The $t_{1/2,1}/t_{1/2,3}$ range of ~ 1–3.5 (vertical dotted lines) provides the preferred $t_{1/2,\beta}/t_{1/2,3}$ range of 0.2–0.8 (horizontal dotted lines); Enz-2208 in mouse (black unfilled circle) and human (black filled circle), PLX038A in mouse (black unfilled square) and PLX038 in human (black filled square)

We can estimate the effect of linker cleavage rates on the relative C_{max}, $C_{max,rel}$, of equal doses of prodrugs, *A* and *B*, that differ only in linker cleavage $t_{1/2,1}$. The ratio of drug concentrations released, as calculated from Eq. 2, approximates the ratio of C_{max} values when $t=0$. Since $V_{d,conj}$, $V_{d,Drug}$, $t_{1/2,2}$, and $t_{1/2,3}$ are constant within a species, all terms except k_1 cancel to give Eq. 4.

$$C_{max,rel} = C_{max,A}/C_{max,B} = k_{1,A}/k_{1,B} \;=\; (t_{1/2,1B})/(t_{1/2,1A}). \tag{4}$$

Thus, at equal doses fast-cleaving linkers that give lower $t_{1/2,1}/t_{1/2,3}$ values result in higher $C_{max,rel}$.

Likewise, we can estimate the effect of linker cleavage rates on the $AUC_{SN\text{-}38}$ by integration of Eq. 2 to give Eq. 5.

$$AUC_{\infty} = [PEG\text{–}Drug]_0 \times (V_{d,conj}/V_{d,drug}) \times \left(k_1/k_2\right) \times \left(1/(k_1 \;+\; k_3)\right). \tag{5}$$

Using Eq. 5, we can define relative AUC values, AUC_{rel}, of the SN-38 released from equal doses of two prodrugs, *A* and *B*, differing only in the release rate k_1 (Eq. 6); note that AUC_{rel} is the ratio of SN-38 utilization efficiencies (Table 1).

$$AUC_{rel} = \frac{AUC_A}{AUC_B} = \frac{k_{1,A}/\left(k_{1,A}+k_3\right)}{k_{1,B}/\left(k_{1,B}+k_3\right)}. \tag{6}$$

Thus, fast-cleaving linkers that give lower $t_{1/2,1}/t_{1/2,3}$ result in higher AUC_{rel}; if $t_{1/2,1}/t_{1/2,3}$ is high, AUC_{rel} is low. Importantly, high AUC_{rel} does not necessarily equate with higher efficacy, since much of the exposure may be "wasted" in the early AUC where drug concentration exceeds the level needed for efficacy.

An acceptable balance of half-life extension and drug utilization is where $t_{1/2,\beta}/t_{1/2,3}$ is between 0.5 and 0.8, and $k_1/(k_1+k_3)$ is between 0.5 and 0.2. These balanced boundaries correspond to $t_{1/2,1}/t_{1/2,3}$ of ~ 1.0–3.5. Thus, in translating the pharmacokinetics of a PEG~SN-38 from one species to another (e.g., mouse to human or vice versa), the cleavage rate k_1 is modified to retain a similar $t_{1/2,1}/t_{1/2,3}$ in the target species within the boundaries of 1–3.5. Once achieved, $t_{1/2,\beta}/t_{1/2,3}$, $k_1/(k_1+k_3)$, and $C_{max,rel}$ are optimized and the process should provide conjugates with similar pharmacokinetic properties in both species.

Linker cleavage $t_{1/2}$ adjustment to optimize $t_{1/2,1}/t_{1/2,3}$ in the mouse

We sought to identify a PEG~SN-38 with a suitable cleavage rate of SN-38 to optimize $t_{1/2,1}/t_{1/2,3}$ in the mouse; we thus studied the pharmacokinetics of conjugates **1A–C** having different modulators (Table 1).

We initially examined the PEG~SN-38 conjugate with a –CN modulator (**1C**), PLX038, which has been extensively studied in the rat [3] and is in Phase 1 clinical trials. With a long cleavage $t_{1/2,1}$ of 360 h and high $t_{1/2,1}/t_{1/2,3}$ of 16, we anticipated this conjugate would perform poorly in the mouse. Indeed, SN-38 release from **1C** was so slow compared to prodrug elimination that $t_{1/2,\beta}$ and $t_{1/2,3}$ were indistinguishable and free SN-38 in plasma was undetectable (Fig. S1C). Clearly, cleavage of **1C** is too slow for efficient use in the mouse.

Next, we examined the $–SO_2Ph$ modulator (**1A**) which showed a $t_{1/2,\beta}$ of only ~ 8 h in the mouse (Fig. S1A) and $t_{1/2,1}$ of 13 h. The $t_{1/2,1}/t_{1/2,3}$ is a very low 0.6 giving high SN-38 utilization and AUC_{rel}, but a low $t_{1/2,\beta}/t_{1/2,3}$ of ~ 0.4 and a high $C_{max,rel}$. Hence, cleavage of the PEG~SN-38 conjugate **1A** is too fast for effective use in the mouse.

Finally, we examined the conjugate **1B** with a $–SO_2Me$ modulator, designated as PLX038A. This showed a $t_{1/2,\beta}$ of 17 h, and a calculated cleavage $t_{1/2,1}$ of~75 h (Fig. 1b). It showed a favorable $t_{1/2,1}/t_{1/2,3}$ of 3.4 and a 25% efficiency of SN-38 utilization (Table 1), some fourfold higher than PLX038. Over 3.6–120 µmol/kg of **1B**, **1B** and released SN-38 showed dose linearity of C_0 and AUC (Table S2). Notably, as in the rat [3], the SN-38G/SN-38 ratio (Fig. 1b) is a very low 0.13. The conjugate **1B**, designated as PLX038A, seems just right for efficacious use in the mouse.

Pharmacokinetic suitability of PEGylated prodrugs of Top1 inhibitors

A number of PEGylated prodrugs of Top1 inhibitors utilize a cleavable ester linkage to release the drug from the carrier [18] and it has been studied in mouse and man. Using the above approach, we compared the pharmacokinetic suitability of Enz-2208—a paradigm of other ester-linked SN-38

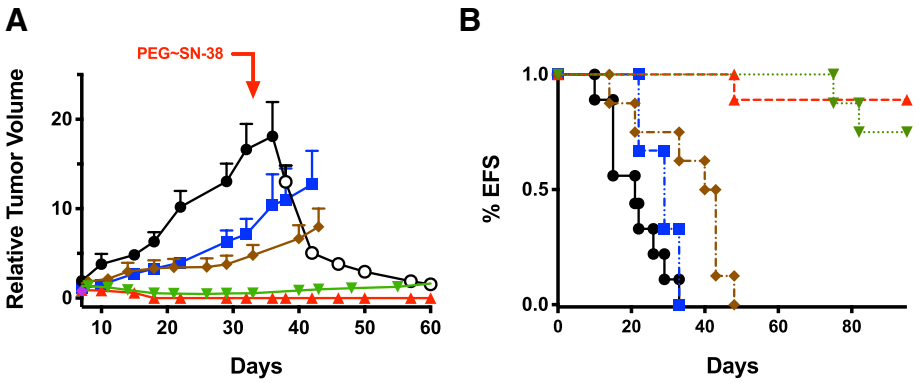

Fig. 3 Effects of PLX038A and CPT-11 on MX-1 tumors. **a** Relative tumor volume vs. time post-dose; vehicle control (black filled circle), and after single i.p. injections of 137 µmol/kg CPT-11 (blue filled square), or 4 (brown filled diamond), 40 (green filled downward triangle) or 120 µmol/kg PLX038A (red filled upward triangle). When the control tumors reached ~ 2000 mm^3, animals were treated with 120 µmol/kg PLX038A (black unfilled circle). Data are mean tumor volumes ± SEM. **b** Event-free survival plot for vehicle control (black filled circle), and after single i.p. injections of 137 µmol/kg CPT-11 (blue filled square), or PLX038A at 120 µmol/kg (red filled upward triangle), 40 µmol/kg (green filled downward triangle), and a combined group (brown filled diamond) of either 13 µmol/kg ($n = 4$) or 4 µmol/kg ($n = 4$). Groups had $n = 8$–9 animals and an event is defined as a fourfold increase in tumor size

prodrugs—with PLX038A, PLX038, and CPT-11 in the mouse and the human. For this purpose, we used parameters given in Table 1 and data from reported dosing schedules of these prodrugs.

In the mouse, Enz-2208 showed $t_{1/2,\beta}$ of ~ 12 h [6, 16], so the $t_{1/2,1}/t_{1/2,3}$ is ~ 1.1, indicating that Enz-2208 has suitable prodrug pharmacokinetics for the mouse. The reported data for released SN-38 at MTDs of Enz-2208 (76 µmol/kg) and CPT-11 (137 µmol/kg) in the mouse (Fig. 3 in Ref. [16]) indicate that the SN-38 from Enz-2208 has a 15-fold higher C_{max} (23 vs. 1.5 µM), a 7-fold longer $t_{1/2}$ (12 vs. 1.7 h), and a 45-fold higher AUC. The pharmacokinetic advantage of Enz-2208 over CPT-11 in the mouse is unambiguous, and the prodrug showed remarkable antitumor efficacy in the mouse.

However, Enz-2208 has a $t_{1/2,\beta}$ of ~ 20 h in the human [17, 19]—only 1.7-fold longer than in the mouse—and an estimated prodrug elimination $t_{1/2,3}$ of 168 h and cleavage $t_{1/2,1}$ of ~ 23 h (from Eq. 3). Thus, $t_{1/2,1}/t_{1/2,3}$ is only 0.13 which indicates SN-38 is released too rapidly to achieve the low C_{max} and extended half-life possible with a longer-acting prodrug. Further, the free SN-38 from 0.6 µmol/kg of the Enz-2208 and 5.6 µmol/kg of the comparator CPT-11 has similar C_{max} values (66 vs. 67 nM), and the $t_{1/2,\beta}$ of SN-38 from Enz-2208 is only ~ twofold longer than that from CPT-11 (21 vs. 10.4 h)—i.e., essentially the same. Thus, although Enz-2208 is effective in the mouse, it is less than an ideal prodrug in the human and the SN-38 that has been formed has pharmacokinetics that are essentially the same as the SN-38 from CPT-11.

In contrast to Enz-2208, the species-independent in vivo cleavage $t_{1/2,1}$ of PLX038 is a long 360 h [3]. Although the $t_{1/2,1}/t_{1/2,3}$ of the prodrug is a very unfavorable 16 in the mouse (Table 1), in the human, the slow linker cleavage and renal elimination of the prodrug provide a favorable $t_{1/2,1}/t_{1/2,3}$ of 2.1 (Table 1). Although the MTD of PLX038 in the human has not yet been reached, the $t_{1/2,\beta}$ obtained from escalating doses is 115 h. By simulating the pharmacokinetics of the SN-38 released from PLX038 such that the AUC_{SN-38} is equal to that of AUC_{SN-38} formed over a 7-day continuous infusion of 22.5 mg/m^2/day CPT-11 (AUC 1.9 µM*h) at its MTD [20], we estimate that the $C_{max,SN-38}$ of a dose of 320 mg/m^2 would be ~ 18 nM, some 3.7-fold lower than the 67 nM $C_{max,SN-38}$ from the 5.6 µmol/kg dose of CPT-11 (Camptosar label). Thus, PLX038 is a poor prodrug in the mouse, but has excellent properties in the human.

Antitumor effects of PLX038A on MX-1

Nude mice with and without MX-1 xenografts were injected i.p. with 120 µmol/kg of PLX038A, the limit imposed by solubility and permitted injection volume. Non-tumor-bearing mice tolerated at least 120 µmol/kg of PLX038A QD or QD×2 without weight loss. MX-1 tumor-bearing mice showed no weight loss after a single dose, but 30% in 14 days after QDx2 dosing (Fig. S3).

Mice bearing ~ 150 mm^3 MX-1 tumors were treated with single i.p. doses of PLX038A, and tumor volumes were measured over time. Tumor volume vs. time and event-free survival plots are shown in Fig. 3a, b; Table S3 provides details of individual tumor growth. The 120 µmol/kg single dose of PLX038A caused shrinkage of the tumor to below 100 mm^3 within ~ 1.5 weeks; 8/9 tumors had a maintained complete response (MCR) for 60–150 days. A single dose of 40 µmol/kg gave tumor shrinkage for ~ 3 weeks and 5/8 animals had a MCR at day 65; 3/8 tumors showed a time

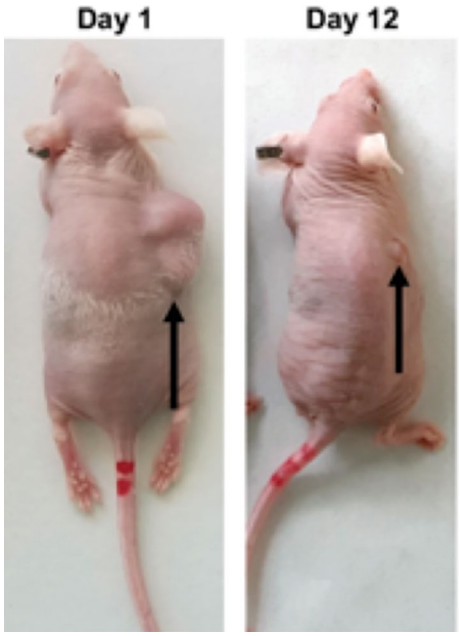

Fig. 4 Mouse with a massive 2600-mm^3 tumor immediately before and 12 days after a single i.p. dose of 120 µmol PLX038A/kg

to progression (TTP) of ~ 4 weeks after dosing but earned classification as a partial response (PR). At doses lower than 40 µmol/kg, there was either tumor shrinkage (at 20 and 30 µmol/kg) over ~ 2–3 weeks followed by exponential regrowth or sustained growth inhibition (at 4–13 µmol/kg) (Fig. S4; Table S3); at 13 µmol/kg, T/C at 21 days (T/C_{21D}) was ~ 0.50. When tumors in the control reached ~ 2000 mm^3, a single 40 µmol/kg (not shown) or 120 µmol/kg dose of PLX038A caused rapid shrinkage of the tumor and CRs (Figs. 3 and 4).

To compare PLX038A to PLX038, each was administered as a single 20 µmol/kg dose.

The T/C_{21D} of PLX038A was 0.17–83% growth inhibition—whereas PLX038 showed a T/C_{21D} of 0.80–20% growth inhibition. The fourfold higher efficacy of PLX038A over PLX038 in the mouse is mirrored by the fivefold higher $C_{max,rel}$ and fourfold higher AUC_{rel} of released SN-38 (Table 1).

To compare PLX038A to CPT-11, a single dose of 137 µmol (80 mg)/kg CPT-11 was administered which resulted in T/C_{21D} of 50%; growth inhibition and event-free survival were inferior to those with 4–13 µmol/kg of PLX038A containing only 1.3–4 mg/kg of SN-38 (Figs. 3a, 4b). The AUC_{SN-38} from this dose of CPT-11 was 7.4 µM*h [16], which is equivalent to the AUC_{SN-38} of a 13 µmol/kg dose of PLX038A (Fig. S2). Hence, in this tumor model, 4–13 µmol SN-38 equivalents of PLX038A were equally effective or superior to 137 µmol SN-38 equivalents of CPT-11.

Discussion

We developed an approach to optimize the pharmacokinetics of a PEG~SN-38 prodrug for a particular species. We then used the approach to assess the suitability of PEGylated prodrugs of SN-38 in the mouse and human, and to develop a variant PEG~SN-38—PLX038A—optimized for use in mouse tumor models. Finally, we demonstrated the remarkable antitumor effects of PLX038A.

To optimize the efficacy of a circulating macromolecular prodrug, the rate of drug release must be balanced with the rate of prodrug renal elimination. Although the drug release rate may or may not be species independent, circulating PEG conjugates have different renal elimination rates in different species that are correlated with the size of the carrier and subject—e.g., for a 40 kDa PEG, ~ 1 day in the mouse, but ~ 7 days in the human [12]. Thus, a prodrug optimal for one species will likely not be for another.

Releasable PEGylated prodrugs such as PEG~SN-38 have distinctive pharmacokinetic properties. Loss of the prodrug occurs by both renal elimination (k_3) and drug release (k_1), and the apparent elimination rate, k_β, of both the prodrug and the released SN-38 is described by $k_1 + k_3$. Since a given PEG~SN-38 will have different elimination rates in different species, prodrug pharmacokinetic parameters that contain k_3—notably k_β, $t_{1/2,1}/t_{1/2,3}$, C_{max}, and exposure—will vary in different species. We propose that the pharmacokinetics of PEG~SN-38 prodrugs can be best translated from one species to another (e.g., mouse to human or vice versa) by modifying the drug release $t_{1/2,1}$ values to retain similar $t_{1/2,1}/t_{1/2,3}$ values—i.e., 1 to 3.5—and adjusting the dose to achieve a desired level of SN-38.

We sought to use this approach to optimize the pharmacokinetics of a PEG~SN-38 conjugate in mouse tumor models. We examined conjugates with different modulators that control the drug release $t_{1/2,1}$ and hence, the $t_{1/12,1}/t_{1/12,3}$ ratio. PLX038, a releasable PEG~SN-38 currently in human clinical trials, has a –CN modulator that confers a long cleavage $t_{1/2,1}$ of 360 h; with an elimination $t_{1/2,3}$ of ~ 1 week, the conjugate shows a favorable $t_{1/2,1}/t_{1/2,3}$ of ~ 2 in humans. However, in the mouse, the lower elimination $t_{1/2,3}$ of ~ 22 h for PEG~SN-38 results in an unfavorably high $t_{1/2,1}/t_{1/2,3}$ of 16 with consequent high $t_{1/2,\beta}/t_{1/2,3}$ and low AUC_{rel}; indeed, SN-38 delivery from PLX038 was so inefficient that it was undetected in plasma. In contrast, with a short drug release $t_{1/2,1}$ of only 13 h, the conjugate with the $–SO_2Ph$ modulator showed an unfavorably low $t_{1/2,1}/t_{1/2,3}$ of 0.6, resulting in a short $t_{1/2,\beta}$ of 9 h and a high $C_{max,rel}$ of released SN-38. Finally, PEG~SN-38 with a $–SO_2Me$ modulator showed a drug release $t_{1/2,1}$ of ~ 75 h, which conferred a $t_{1/2,1}/t_{1/2,3}$ of 3.4 in the mouse—close to that of PLX038 in humans—and

provided a $t_{1/2,\beta}$ of 17 h to the released SN-38. The prodrug PLX038A provided a good balance of $t_{1/2,\beta}/t_{1/2,3}$ and SN-38 exposure in the mouse that are analogous to PLX038 in the human.

In addition to half-life optimization, the β-eliminative linkers confer other advantages to PLX038 and PLX038A compared to CPT-11. In humans and rodents, the dose of CPT-11 does not correlate with the C_{max} and AUC values for the active metabolite SN-38 [21–24]. In contrast, there is an excellent correlation of dose with C_{max} and AUC of the released SN-38 over a 30-fold concentration range of PLX038A. This is an expected consequence of the simple, chemically controlled β-elimination that directly generates SN-38 from the prodrug. Additionally, with CPT-11, there is massive liver exposure to SN-38 that is manifested by a high SN-38G/SN-38 ratio of ≥ 3.0, and there is a strong correlation between SN-38G AUC and GI toxicity [25]. In contrast, the SN-38G/SN-38 ratio after treatment with PLX038 [14] or PLX038A is ≤ 0.2 indicating very low liver exposure of the released SN-38 and explaining the low GI toxicity of these prodrugs.

Our model allowed us to analyze the pharmacokinetic suitability of previous PEGylated Top1 inhibitor prodrugs. Superior efficacy of Top1 inhibitors is usually determined by favorable comparison of antitumor effects to a "gold-standard" Top1 inhibitor, such as CPT-11. The objective of designing these PEGylated prodrugs was to increase the circulating lifetime of SN-38 and, thereby, sustain Top1 inhibition for longer periods [26]. Indeed, maintaining low levels of Top1 inhibitors—CPT-11 or Topotecan—within their therapeutic windows by multiple low doses over a protracted period showed greater antitumor activity and less toxicity than single bolus therapy [27, 28]. Previous PEGylated SN-38 prodrugs consisted of PEG attached to SN-38 or CPT-11 via an ester bond that hydrolyzed with an in vitro $t_{1/2}$ of ≤ 24 h [10, 18, 26]. Since in vivo ester hydrolysis may be faster (e.g., through esterases) but not slower than in vitro hydrolysis, the in vitro cleavage $t_{1/2}$ represents an upper limit for in vivo drug release $t_{1/2,1}$ and $t_{1/2,\beta}$ of the released drug.

As an example, Enz-2208 is a releasable PEG_{40kDa}~SN-38 that is structurally similar to PLX038 and PLX038A except it undergoes ester hydrolysis rather than β-elimination to release free SN-38. The initial efficacy studies of Enz-2208 were performed in tumor-bearing mice, where the conversion of CPT-11 to SN-38 is rapid due to high plasma carboxylesterase, and thus the $t_{1/2,\beta}$ for the SN-38 formed is atypically short [29, 30]. Enz-2208 showed remarkable efficacy in mouse xenografts compared to CPT-11 [6, 16] which is attributable to the significantly lower C_{max}, longer half-life, and exposure of the released SN-38. However, the efficacy in mouse xenografts did not translate to human cancer patients. In a signal-seeking randomized Phase 2 study of cetuximab plus Enz-2208 or CPT-11 in advanced colorectal cancer, there was no significant difference on progression free or overall survival [7]. Without a signal indicating benefit over the standard of care comparator CPT-11, further development of Enz-2208 was abandoned.

One explanation for the non-superiority of Enz-2208 over the comparator CPT-11 in human cancer is simply that the C_{max} and elimination $t_{1/2}$ values of the released SN-38 from these two prodrugs were—within error—the same [17, 31]. In contrast, the $t_{1/2,\beta}$ of the SN-38 released from PLX038 in the human is ~ tenfold longer, and its C_{max} is substantially lower than that from CPT-11. The still unanswered question of whether prolonging the half-life of a Top1 inhibitor will be of benefit in treating cancers in humans remains to be resolved.

Since all ester-linked prodrugs of Top1 inhibitors have similar half-lives for drug release, their limited antitumor efficacy in the human can be explained by the same rationale as for Enz-2208. Likewise, the antibody drug conjugate (ADC) sacituzumab govitecan has a carbonate linkage to SN-38 that has cleavage half-life of about 20 h [32]—almost identical to that of Enz-2208. The levels of free SN-38 released by hydrolysis from a 10 mg/kg dose of sacituzumab govitecan exceed 200 nM, and the AUC is ~ 7.6 μM*h—both significantly higher than the values observed at the MTD of Enz-2208 ($C_{max,SN-38}$ ~ 70 nM, AUC ~ 2.5 μM*h) or a high Q3Wk 350 mg/m^2 dose of CPT-11 ($C_{max,SN-38}$ ~ 160 nM, AUC ~ 1.2 μM*h). Thus, the pharmacokinetics of the SN-38 released by sacituzumab govitecan resemble that of high doses of Enz-2208 or CPT-11 and its antitumor effects may reflect its ability to serve as a releasable prodrug of SN-38 as well as, or instead of, the mechanism normally associated with an ADC.

PLX038A showed remarkable antitumor growth effects on the MX-1 xenograft, a CPT-11 and PARP inhibitor-sensitive triple negative breast cancer possessing a BRCA1 defect [33, 34]. A single dose of only 13 μmol/kg PLX038A inhibited growth with a T/C_{21D} of 50%, and single doses of 40–120 μmol/kg PLX038A caused tumor shrinkage and cures. Perfectly aligned with the fourfold higher AUC_{SN-38}, at equivalent doses PLX038A was fourfold more effective in tumor growth inhibition than PLX038. PLX038A also showed clear superiority over the "gold-standard" Top1 inhibitor CPT-11; growth inhibition, event-free survival, and the AUC_{SN-38} of 4–13 μmol/kg PLX038A was equivalent to 137 μmol/kg of CPT-11. Further, PLX038A is well tolerated at doses up to ~ tenfold higher than the equally effective MTD dose of CPT-11. Clearly, with the MX-1 xenograft, PLX038A is significantly more effective and less toxic than CPT-11.

Strikingly, at doses of 40 and 120 μmol/kg, PLX038A caused precipitous shrinkage of massive ≥ 2000 mm^3 MX-1 tumors to < 100 mm^3. We are unaware of any single-dose agent that causes tumor reduction of this magnitude over

a short period. A notable feature of PLX038A is that it is effective after administering only a single, non-toxic dose. With a half-life of 22 h, ~ 95% of the drug is cleared within 4 days—less than the doubling time of the tumor such that many cells will not be exposed to effective levels of PLX038A by the time they enter Top1-sensitive S-phase. Nonetheless, we observe complete shrinkage of large tumors over a period of more than 20 days post-dose, indicating continued exposure of tumor cells to PLX038A well beyond the period required for systemic clearance. We posit that there is tumor retention of the drug, such as via the EPR effect that has been observed with similar PEGylated Top1 prodrugs [6, 16]. A future report will detail and analyze the remarkable antitumor effects of PLX038A as a single agent and in combination with inhibitors of DNA damage responses.

Acknowledgements We thank Julia Malato, Fernando Salangsang, Paul Phojanakong for performing the xenograft studies.

Compliance with ethical standards

Conflict of interest Shaun D. Fontaine, Ralph Reid, Gary W. Ashley, and Daniel V. Santi are all employees and shareholders of ProLynx LLC. Byron Hann is an employee of University of California, San Francisco.

Research involving animals All studies involving animals were in accordance with the ethical standards of the institution at which the studies were conducted.

References

1. Mathijssen RH, van Alphen RJ, Verweij J, Loos WJ, Nooter K, Stoter G, Sparreboom A (2001) Clinical pharmacokinetics and metabolism of irinotecan (CPT-11). Clin Cancer Res 7(8):2182–2194
2. Slatter JG, Schaaf LJ, Sams JP, Feenstra KL, Johnson MG, Bombardt PA, Cathcart KS, Verburg MT, Pearson LK, Compton LD, Miller LL, Baker DS, Pesheck CV, Lord RS 3rd (2000) Pharmacokinetics, metabolism, and excretion of irinotecan (CPT-11) following I.V. infusion of [(14)C]CPT-11 in cancer patients. Drug Metab Dispos 28(4):423–433
3. Santi DV, Schneider EL, Ashley GW (2014) Macromolecular prodrug that provides the irinotecan (CPT-11) active-metabolite SN-38 with ultralong half-life, low C(max), and low glucuronide formation. J Med Chem 57(6):2303–2314. https://doi.org/10.1021/jm401644v
4. Maeda H, Tsukigawa K, Fang J (2016) A retrospective 30 years after discovery of the enhanced permeability and retention effect of solid tumors: next-generation chemotherapeutics and photodynamic therapy-problems, solutions, and prospects. Microcirculation 23(3):173–182. https://doi.org/10.1111/micc.12228
5. Zander SA, Sol W, Greenberger L, Zhang Y, van Tellingen O, Jonkers J, Borst P, Rottenberg S (2012) EZN-2208 (PEG-SN38) overcomes ABCG2-mediated topotecan resistance in BRCA1-deficient mouse mammary tumors. PLoS One 7(9):e45248. https://doi.org/10.1371/journal.pone.0045248
6. Sapra P, Kraft P, Mehlig M, Malaby J, Zhao H, Greenberger LM, Horak ID (2009) Marked therapeutic efficacy of a novel polyethylene glycol-SN38 conjugate, EZN-2208, in xenograft models of B-cell non-Hodgkin's lymphoma. Haematologica 94(10):1456–1459. https://doi.org/10.3324/haematol.2009.008276
7. Garrett CR, Bekaii-Saab TS, Ryan T, Fisher GA, Clive S, Kavan P, Shacham-Shmueli E, Buchbinder A, Goldberg RM (2013) Randomized phase 2 study of pegylated SN-38 (EZN-2208) or irinotecan plus cetuximab in patients with advanced colorectal cancer. Cancer 119(24):4223–4230. https://doi.org/10.1002/cncr.28358
8. Matsumura Y (2011) Preclinical and clinical studies of NK012, an SN-38-incorporating polymeric micelles, which is designed based on EPR effect. Adv Drug Deliv Rev 63(3):184–192. https://doi.org/10.1016/j.addr.2010.05.008
9. Ri M, Suzuki K, Iida S, Hatake K, Chou T, Taniwaki M, Watanabe N, Tsukamoto T (2017) A phase I/II study for dose-finding, and to investigate the safety, pharmacokinetics and preliminary efficacy of NK012, an SN-38-incorporating macromolecular polymeric micelle, in patients with multiple myeloma. Intern Med. https://doi.org/10.2169/internalmedicine.9567-17
10. Hoch U, Staschen CM, Johnson RK, Eldon MA (2014) Nonclinical pharmacokinetics and activity of etirinotecan pegol (NKTR-102), a long-acting topoisomerase 1 inhibitor, in multiple cancer models. Cancer Chemother Pharmacol 74(6):1125–1137. https://doi.org/10.1007/s00280-014-2577-7
11. Jameson GS, Hamm JT, Weiss GJ, Alemany C, Anthony S, Basche M, Ramanathan RK, Borad MJ, Tibes R, Cohn A, Hinshaw I, Jotte R, Rosen LS, Hoch U, Eldon MA, Medve R, Schroeder K, White E, Von Hoff DD (2013) A multicenter, phase I, dose-escalation study to assess the safety, tolerability, and pharmacokinetics of etirinotecan pegol in patients with refractory solid tumors. Clin Cancer Res 19(1):268–278. https://doi.org/10.1158/1078-0432.CCR-12-1201
12. Santi DV, Schneider EL, Reid R, Robinson L, Ashley GW (2012) Predictable and tunable half-life extension of therapeutic agents by controlled chemical release from macromolecular conjugates. Proc Natl Acad Sci USA 109(16):6211–6216. https://doi.org/10.1073/pnas.1117147109
13. Henise J, Hearn BR, Ashley GW, Santi DV (2015) Biodegradable tetra-PEG hydrogels as carriers for a releasable drug delivery system. Bioconjug Chem 26(2):270–278. https://doi.org/10.1021/bc5005476
14. Schneider EL, Robinson L, Reid R, Ashley GW, Santi DV (2013) beta-eliminative releasable linkers adapted for bioconjugation of macromolecules to phenols. Bioconjug Chem 24(12):1990–1997. https://doi.org/10.1021/bc4002882
15. Houghton PJ, Morton CL, Tucker C, Payne D, Favours E, Cole C, Gorlick R, Kolb EA, Zhang W, Lock R, Carol H, Tajbakhsh M, Reynolds CP, Maris JM, Courtright J, Keir ST, Friedman HS, Stopford C, Zeidner J, Wu J, Liu T, Billups CA, Khan J, Ansher S, Zhang J, Smith MA (2007) The pediatric preclinical testing program: description of models and early testing results. Pediatr Blood Cancer 49(7):928–940. https://doi.org/10.1002/pbc.21078
16. Sapra P, Zhao H, Mehlig M, Malaby J, Kraft P, Longley C, Greenberger LM, Horak ID (2008) Novel delivery of SN38 markedly inhibits tumor growth in xenografts, including a camptothecin-11-refractory model. Clin Cancer Res 14(6):1888–1896. https://doi.org/10.1158/1078-0432.CCR-07-4456
17. Kurzrock R, Goel S, Wheler J, Hong D, Fu S, Rezai K, Morgan-Linnell SK, Urien S, Mani S, Chaudhary I, Ghalib MH, Buchbinder A, Lokiec F, Mulcahy M (2012) Safety, pharmacokinetics, and activity of EZN-2208, a novel conjugate of polyethylene glycol and SN38, in patients with advanced malignancies. Cancer 118(24):6144–6151. https://doi.org/10.1002/cncr.27647
18. Koizumi F, Kitagawa M, Negishi T, Onda T, Matsumoto S, Hamaguchi T, Matsumura Y (2006) Novel SN-38-incorporating

polymeric micelles, NK012, eradicate vascular endothelial growth factor-secreting bulky tumors. Cancer Res 66(20):10048–10056. https://doi.org/10.1158/0008-5472.CAN-06-1605
19. Patnaik A, Papadopoulos KP, Tolcher AW, Beeram M, Urien S, Schaaf LJ, Tahiri S, Bekaii-Saab T, Lokiec FM, Rezai K, Buchbinder A (2013) Phase I dose-escalation study of EZN-2208 (PEG-SN38), a novel conjugate of poly(ethylene) glycol and SN38, administered weekly in patients with advanced cancer. Cancer Chemother Pharmacol 71(6):1499–1506. https://doi.org/10.1007/s00280-013-2149-2
20. Masi G, Falcone A, Di Paolo A, Allegrini G, Danesi R, Barbara C, Cupini S, Del Tacca M (2004) A phase I and pharmacokinetic study of irinotecan given as a 7-day continuous infusion in metastatic colorectal cancer patients pretreated with 5-fluorouracil or raltitrexed. Clin Cancer Res 10(5):1657–1663
21. Rothenberg ML, Kuhn JG, Burris HA 3rd, Nelson J, Eckardt JR, Tristan-Morales M, Hilsenbeck SG, Weiss GR, Smith LS, Rodriguez GI et al (1993) Phase I and pharmacokinetic trial of weekly CPT-11. J Clin Oncol 11(11):2194–2204. https://doi.org/10.1200/JCO.1993.11.11.2194
22. Rothenberg ML, Kuhn JG, Schaaf LJ, Rodriguez GI, Eckhardt SG, Villalona-Calero MA, Rinaldi DA, Hammond LA, Hodges S, Sharma A, Elfring GL, Petit RG, Locker PK, Miller LL, von Hoff DD (2001) Phase I dose-finding and pharmacokinetic trial of irinotecan (CPT-11) administered every two weeks. Ann Oncol 12(11):1631–1641
23. Rouits E, Guichard S, Canal P, Chatelut E (2002) Non-linear pharmacokinetics of irinotecan in mice. Anticancer Drugs 13(6):631–635
24. Stewart CF, Zamboni WC, Crom WR, Houghton PJ (1997) Disposition of irinotecan and SN-38 following oral and intravenous irinotecan dosing in mice. Cancer Chemother Pharmacol 40(3):259–265. https://doi.org/10.1007/s002800050656
25. Xie R, Mathijssen RH, Sparreboom A, Verweij J, Karlsson MO (2002) Clinical pharmacokinetics of irinotecan and its metabolites in relation with diarrhea. Clin Pharmacol Ther 72(3):265–275. https://doi.org/10.1067/mcp.2002.126741
26. Zhao H, Rubio B, Sapra P, Wu D, Reddy P, Sai P, Martinez A, Gao Y, Lozanguiez Y, Longley C, Greenberger LM, Horak ID (2008) Novel prodrugs of SN38 using multiarm poly(ethylene glycol) linkers. Bioconjug Chem 19(4):849–859. https://doi.org/10.1021/bc700333s
27. Houghton PJ, Cheshire PJ, Hallman JD 2nd, Lutz L, Friedman HS, Danks MK, Houghton JA (1995) Efficacy of topoisomerase I inhibitors, topotecan and irinotecan, administered at low dose levels in protracted schedules to mice bearing xenografts of human tumors. Cancer Chemother Pharmacol 36(5):393–403. https://doi.org/10.1007/BF00686188
28. Guichard S, Montazeri A, Chatelut E, Hennebelle I, Bugat R, Canal P (2001) Schedule-dependent activity of topotecan in OVCAR-3 ovarian carcinoma xenograft: pharmacokinetic and pharmacodynamic evaluation. Clin Cancer Res 7(10):3222–3228
29. Morton CL, Wierdl M, Oliver L, Ma MK, Danks MK, Stewart CF, Eiseman JL, Potter PM (2000) Activation of CPT-11 in mice: identification and analysis of a highly effective plasma esterase. Cancer Res 60(15):4206–4210
30. Morton CL, Iacono L, Hyatt JL, Taylor KR, Cheshire PJ, Houghton PJ, Danks MK, Stewart CF, Potter PM (2005) Activation and antitumor activity of CPT-11 in plasma esterase-deficient mice. Cancer Chemother Pharmacol 56(6):629–636. https://doi.org/10.1007/s00280-005-1027-y
31. Chabot GG (1997) Clinical pharmacokinetics of irinotecan. Clin Pharmacokinet 33(4):245–259. https://doi.org/10.2165/00003088-199733040-00001
32. Ocean AJ, Starodub AN, Bardia A, Vahdat LT, Isakoff SJ, Guarino M, Messersmith WA, Picozzi VJ, Mayer IA, Wegener WA, Maliakal P, Govindan SV, Sharkey RM, Goldenberg DM (2017) Sacituzumab govitecan (IMMU-132), an anti-Trop-2-SN-38 antibody-drug conjugate for the treatment of diverse epithelial cancers: safety and pharmacokinetics. Cancer 123(19):3843–3854. https://doi.org/10.1002/cncr.30789
33. Boerner JL, Nechiporchik N, Mueller KL, Polin L, Heilbrun L, Boerner SA, Zoratti GL, Stark K, LoRusso PM, Burger A (2015) Protein expression of DNA damage repair proteins dictates response to topoisomerase and PARP inhibitors in triple-negative breast cancer. PLoS One 10(3):e0119614. https://doi.org/10.1371/journal.pone.0119614
34. Shen Y, Rehman FL, Feng Y, Boshuizen J, Bajrami I, Elliott R, Wang B, Lord CJ, Post LE, Ashworth A (2013) BMN 673, a novel and highly potent PARP1/2 inhibitor for the treatment of human cancers with DNA repair deficiency. Clin Cancer Res 19(18):5003–5015. https://doi.org/10.1158/1078-0432.CCR-13-1391

Supplementary Information

Species-specific optimization of PEG~SN-38 prodrug pharmacokinetics and anti-tumor effects in a triple-negative BRCA1-deficient xenograft

Shaun D. Fontaine, Byron Hann, Ralph Reid, Gary W. Ashley and Daniel. V. Santi*

Table of Contents

I. General

PEG_{40kDa}-$[NH_2]_4$ (Sunbright PTE-400PA) was purchased from NOF America, and SN-38 was from Genegobio. All other commercially available chemicals were purchased as reagent grade and used without further purification. Solutions of PEG~SN-38 (**1A-1D**) were quantified by UV absorbance using ε_{363nm} = 22,500 M^{-1} cm^{-1} at pH 7. Solutions of SN-38 were quantified using ε_{414nm} = 27,500 M^{-1} cm^{-1} at pH 10 (1). Doses of PEG~SN38 are reported with respect to the amount of conjugated SN-38 delivered – i.e. 120 µmol/kg is 120 µmol SN-38/kg delivered as PEG~SN-38.

Unless otherwise specified, HPLC analyses were performed on either a Shimadzu LC-20AD HPLC system equipped with an SPD-M20A diode array detector and RF-10AXL fluorescence detector or an Agilent Series 1100 HPLC system equipped with an Agilent G1315A diode array detector and an Alltech 3300 ELSD. Both HPLC systems were fitted with a Phenomenex Jupiter 5 µm C18 column (300 Å, 150 x 4.6 mm). Synthetic reactions were monitored using an HPLC mobile phase of H_2O/0.1% TFA and MeCN/0.1% TFA. UV-vis data were acquired on a Hewlett Packard 8453 UV-vis spectrometer. NMR spectra were acquired at the UCSF Small Molecule Discovery Center using a Bruker Avance 300 MHz spectrometer. LCMS analyses were obtained at the UCSF Small Molecule Discovery center core facility using a Waters Micromass ZQTM equipped with a Waters 2795 Separation Module and a Waters 296 Photodiode Array detector.

Pharmacokinetic studies (described below) were performed at Agilux Laboratories (now Charles River) in Worcester, MA. Tolerability studies were performed at Murigenics (Vallejo, CA), and

tumor studies were conducted at the UCSF Preclinical Therapeutics Core Facility (San Francisco, CA).

II. Synthesis

PEG~SN-38 conjugates. Over the course of these studies, PEG~SN-38 conjugates were prepared containing amide and triazole connectors to tether linkers to the carrier (2). Amide connections were made by coupling $PEG_{40kDa}(CO\text{-}HSE)_4$ with NH_2-linker-SN-38; this method was used early in this study but it suffered from the hydrolytic lability of the activated PEG. Triazole connectors were prepared by coupling a $PEG_{40kDa}(cyclooctyne)_4$ with azide-terminated linker-SN-38 via SPAAC; this approach allows storage of precursors and simple high yield couplings. The cyclooctynes used included DBCO, MFCO and 5-hydroxy-cyclooctyne (5HCO). Currently, we favor use of 5-hydroxy-cyclooctyne for SPAAC because of its cost-effectiveness, stability, and ease of use. The preparation of PEG~SN-38 with amide and DBCO connectors have been published (2). Preparation of $PEG(MFCO)_4$ and its coupling to azido-linker-drug conjugates followed reported procedures (3). Below are procedures that describe preparation of PEG~SN-38 conjugates with 5-hydroxy-cycloctyne connectors.

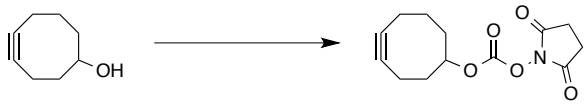

S1

***O*-Cyclooct-4-yn-1-yl-*O*'-succinimidyl carbonate (5-HCO-HSC; S1).** A 250-mL, round-bottomed flask was charged with 5-hydroxycyclooctyne (4) (3.3 g, 26.6 mmol, 1.0 equiv, 0.2 M final concentration), CH_2Cl_2 (122 mL), DSC (13.6 g, 53.2 mmol, 2 equiv, 0.4 M final concentration), Et_3N (8.11 mL, 58.5 mmol, 2.2 equiv, 0.4 M final concentration), and DMAP (650 mg, 5.32 mmol, 0.2 equiv, 0.04 M final concentration). The reaction mixture was stirred at ambient temperature for 24 h. The reaction mixture was diluted with CH_2Cl_2 (300 mL) and washed with saturated $NaHCO_3$, H_2O, 5% aqueous $KHSO_4$, H_2O, brine (100 mL each). The organic phases were concentrated and filtered through a cotton plug onto a silica gel column (120 g silica gel cartridge). Gradient elution (10%, 20%, 30%, 40%, 50% (200 mL each) acetone/hexanes) afforded 6.73 g (88% purity by weight; by ^1H NMR = 5.92 g, 22.3 mmol, 84% calculated yield) of desired HSC **S1** as a yellow oil. ^1H NMR ($CDCl_3$, 300 MHz) δ ppm 4.79 (dd, *J*=9.4, 5.3 Hz, 1 H), 2.81 (s, 4 H), 2.28 - 2.56 (m, 2 H), 2.04 - 2.28 (m, 6 H), 1.82 - 2.03 (m, 2 H). ^{13}C NMR ($CDCl_3$, 300 MHz) δ 168.8, 150.9, 94.1, 92.8, 87.8, 39.6, 37.8, 30.8, 29.8, 25.4, 19.9, 17.5.

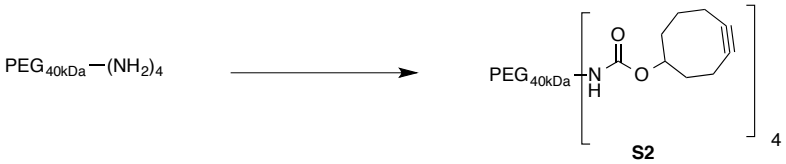

S2

PEG_{40kDa}-[5HCO]$_4$ (S2). A 500-mL, heat-gun dried, round-bottomed flask equipped with a stir bar, rubber septum, and nitrogen inlet was charged with PEG_{40kDa} tetramine (PEG_{40kDa}-$[NH_2]_4$) (19.4 g, 0.479 mmol PEG, 1.92 mmol NH_2, 1.0 equiv, 20 mM NH_2 final concentration), MeCN (81 mL), and iPr_2NEt (0.40 mL, 2.3 mmol, 1.2 equiv, 24 mM final concentration). A solution of 5HCO-HSC (**S1**) (150 mM in MeCN, 15.3 mL, 2.30 mmol, 1.2 equiv, 24 mM final concentration) was added via syringe over 2 min. The reaction mixture was stirred at ambient temperature for 1 h. Reaction progress was monitored by C18 HPLC (20-80% B, ELSD) and showed the starting tetramine (R_T = 8.99 min) converting to a less polar product ($(5HCO)_4$; R_T= 9.76 min) via

three intermediates. Acetic anhydride (0.18 mL, 1.92 mmol, 1.0 equiv, 20 mM final concentration) was added, the reaction mixture was stirred at ambient temperature for 5 min, and concentrated to an approximate volume of 20 mL. The crude product was then dissolved in THF (200 mL) and precipitated by addition into MTBE (1 L). The resulting suspension was stirred at ambient temperature for 10 min and the resulting solids were collected by vacuum filtration on a sintered glass funnel, washed with MTBE (3x100 mL), and dried under high vacuum for 20 min to afford 20.1 g (1.96 mmol, 102% yield) of the desired product (**S2**) as a white solid. The product was immediately dissolved in MeCN (63 mL). Cyclooctyne content was measured by reaction of an aliquot with 2 equiv of PEG_7-N_3 and back-titration of unreacted azide with DBCO: (expected: 23.5 mM, found: 24.5 ± 1.5 mM (106%). C18 HPLC was monitored by ELSD: 99% (96% PEG-$[5HCO]_4$, 4% PEG-$[5HCO]_3$.

PLX038A (1B)

PLX038A (PEG~SN-38, Mod = SO_2Me) (**1B**). A 250-mL round-bottomed flask equipped with a stir bar, rubber septum, and nitrogen inlet was charged a solution PEG-$[5HCO]_4$ (24.5 mM cyclooctyne in MeCN, 73 mL, 1.79 mmol, 1.0 equiv, 25 mM final cyclooctyne concentration) and azido-linker(SO_2Me)-SN-38 (**S3)** (1.8 g, 90% pure by weight, 1.88 mmol, 1.05 equiv, 25.7 mM final azide concentration) (2). The reaction mixture was stirred at 37 °C for 24 h. Additional azido-linker(SO_2Me)-SN-38 (170 mg, 90% pure by weight, 0.178 mmol, 0.1 equiv) was added and the reaction mixture was stirred for an additional 24 h at 37 °C. C18 HPLC (0-100%B, 370 nm) analysis of the reaction solution showed a mixture of desired product (82%), unreacted azido-linker-SN-38 (10%), and free SN-38 (8%). The reaction mixture was concentrated to a yellow residue then dissolved in THF (200 mL). The product was precipitated by addition to vigorously stirring MTBE (1 L). The resulting suspension was stirred at ambient temperature for 20 min then the solids were collected by vacuum filtration. C18 HPLC analysis as above showed purity of the isolated material contained 95% desired product (4% unreacted azido-linker-SN-38 and 1% free SN-38). The precipitation was repeated once and the collected solids were dried under high vacuum to give 16.8 g (0.37 mmol conjugate, 1.51 mmol SN-38, 84% yield) of the desired product as a pale yellow solid. C18 HPLC was monitored at 370 nm: 98%.

III. Pharmacokinetic studies

1. Drug administration and analysis: Serial micro-sampling pharmacokinetic assays in mice were performed by Agilux Laboratories (Charles River) using male CD-1 mice ~25 g in weight (N = 3-4).

Dosing solutions of PEG~SN-38 (**1A**-**1D**) contained ≤2 mM conjugate (≤7.9 mM SN-38) in isotonic 10 mM NaOAc, pH 5.0, and were sterile filtered through a 0.2 µm syringe filter. Injections were performed i.p. at 5-15 mL/kg body weight to deliver 3.6, 11.4, 30.3, 40.0, or 120 µmol/kg. Blood samples (~30 µL) were collected from each animal via tail snip at 0, 1, 2, 4, 8, 16, 32, 64, and 104 h and stabilized by the addition of 0.1% Pluronic F68 and (5) 10 mM bis(4-nitrophenyl) phosphate (6,7) and 20% DMA/1 M citrate pH 4.9 (3 µL). Samples were stored on ice (<1 h) and centrifuged (3,200xg at 5 °C) to give 5-20 µL plasma samples that were stored at -80 °C until analysis.

HPLC Analysis (PEG~SN-38): Plasma samples were thawed on ice and an aliquot (8 µL) was removed, treated with MeOH/0.5% AcOH containing 15 µM α-DNP-Lysine as an internal standard (40 µL), and centrifuged (16,000xg,10 min, 4 °C). The supernatant was removed and further diluted with H_2O/0.5% AcOH (150 µL). Samples (150 µL injection) were analyzed by C18 HPLC (Phenomenex Jupiter C18, 300 Å, 150 mm x 4.6 mm column, column heated at 40 °C, autosampler cooled to 4 °C). Samples were analyzed on the following gradient consisting of H_2O/0.1% TFA (Buffer A) and MeCN/0.1% TFA (Buffer B): 0%B for 1 min, 0-100%B for 10 min, 100%B for 2 min, 100-0%B for 1 min, 0% B for 2 min. Sample elution was monitored with a diode array detector (380 nm) and a fluorescence detector (ex: 370 nm; em: 534 nm for 0-7.4 min, em: 550 nm for 7.4-15 min). R_T: PEG~SN-38: 9.3 min; SN-38: 8.0 min; SN-38G: 7.0 min. LLOQ: PEG~SN-38 = 6 pmol; SN-38 = 0.27 pmol; SN-38G = 0.04 pmol.

2. Pharmacokinetics of PEG~SN-38 analogs 1A-1D:

Concentration vs time (C vs t) data for PEG~SN-38, SN-38, and SN-38G (when detected) were fit to a two-compartment model (**Scheme 3**, text) to determine rate constants k_a and (k_1+k_3) using Eqs. 1-4 in Prism.

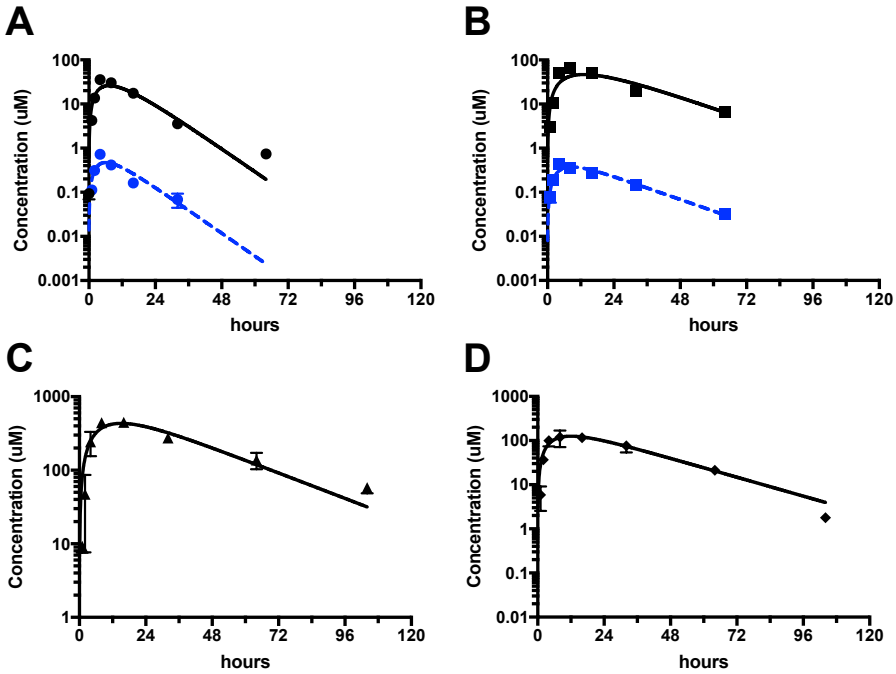

Figure S1. C vs t curves of PEG~SN-38 (black, solid) and SN-38 (blue, dash) for conjugates **1A-D** after i.p. injection**.** Data shows the average ± SEM and lines are least squares best-fits to Eq. 1 (i.p.) and data weighted by 1/SD^2. A) Mod = SO_2Ph (**1A,**●); B) Mod = SO_2Me (**1B,** ■); C) Mod = CN (**1C,** ▲); D) Mod = H (**1D,** ◆).

Table S1. PK Parameters of PEG~SN-38 analogs **1A-1D**[a]

PEG-SN-38	**1A**	**1B PLX038A**	**1C PLX038**	**1D**
Mod	-SO_2Ph	-SO_2Me	-CN	-H
dose, μmol/kg	8.4	40	83.6	39.7
PEG-SN-38				
C_0, μM[b]	56	460	1007	556
Cmax, μM[c]	36	351	447	380
V_d, L/kg[d]	0.36	0.09	0.15	0.08
V_z, L/kg[e]	0.15	0.09	0.08	0.07
$t_{1/2,\alpha}$, h		3.8	~0.2	4.7
$t_{1/2,\beta}$, h	8.9	16.8	28.7	22.1
AUC, μM*h	300	10438	22400	16700
SN-38				
C_{max}, μM	0.72	0.41		
C_0, μM	1.01	1.63		
AUC, μM*h	3.3	13.6		
SN-38G				
C_{max}, μM		0.093		
C_0, μM		0.092		
AUC, μM*h		2.043		

[a] PK parameters derived from fits of pharmacokinetic data to either a biexponential (1B-1D; $y=C_0*((\exp(-k_1*t)-\exp(-k_2*t))$ or single exponential equations in Prism. [b] C_0 is the theoretical concentration at t=0 obtained by extrapolation of the $t_{1/2,\beta}$ and calculated in the above equation. [c] C_{max} is maximum observed concentrated at t_{max}. [d] V_d calculated as Dose/C_0. [e] V_z calculated as (Dose/(k*AUC)).

3. Dose Linearity of AUC and C_0 for PLX038A (1B)

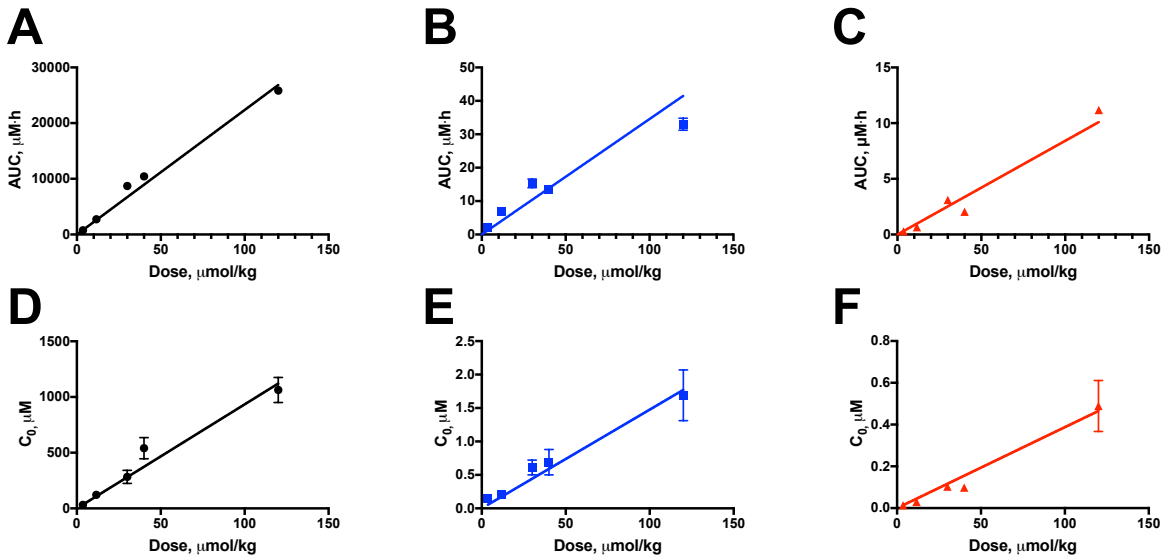

Figure S2. AUC and C_0 as a function of dose. Data is plotted as Average ± SEM. A) AUC PLX038A (**1B**); $R^2 = 0.981$; B) AUC SN-38; $R^2 = 0.838$; C) AUC SN-38G; $R^2 = 0.938$. D) C_0 PLX038A (**1B**); $R^2 = 0.954$; E) C_0 SN-38; $R^2 = 0.965$; F) SN-38G; $R^2 = 0.972$.

IV. Anti-tumor activity of PLX038A in the MX-1 murine xenograft

1. Tolerability of PLX038A in nude mice: Non-tumor bearing, nude male mice (Taconic NCRNU-M nu/nu, ~25 g starting weight, N=3) or MX-1 bearing nude female mice (Taconic NCRNU-F nu/nu, ~25 g starting weight , N=3) were administered 120 µmol/kg of PLX038A (**1B**) at 10-13 mL/kg i.p. as a single dose (QDx1), once daily for 2 days (QDx2), or twice daily for three days (BIDx3). Body weights were measured periodically and are summarized in **Fig. S3**. Mice were sacrificed if a weight loss of >20% was observed.

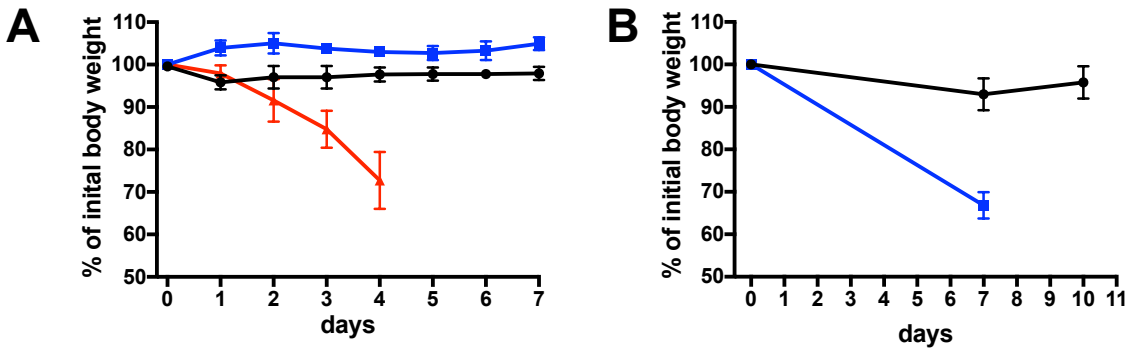

Figure S3. MTD experiments measuring body weight over time. A) Tolerability of PLX038A in nude, non-tumor bearing mice (male, NCRNU-M, nu/nu) receiving: 120 µmol/kg QD (●), 120 µmol/kg QDx2 (■), and 120 µmol/kg BIDx3 (▲). Significant body weight loss was observed for mice receiving 120 µmol/kg BIDx3 (▲) which resulted in the death of 1 mouse on day 2, the remaining 2 mice were euthanized on day 4. B) Body weight for nude, MX-1 tumor-bearing mice (female, NCRNU-F, nu/nu) receiving 120 µmol/kg QD (●) and 120 µmol/kg QDx2 (■). All mice receiving 120 µmol/kg QDx2 PLX038A (■) were euthanized on day 7 due to body weight loss.

2. Preparation of murine MX-1 xenografts: The MX-1 human triple-negative breast carcinoma cell line was obtained from Charles River Labs (Frederick, Maryland). Cells were cultured in RPMI-1640, 10% FBS and 1% 2 mM L-glutamine at 37 °C in 95% air/5% CO_2 atmosphere. (8) These cells had been passaged for <6 months at the time of the experiments described in this report.

Female NCr nude mice (NCRNU-F, nu/nu, NCrTac:NCr-*Foxn1*^{nu}; ~6-7 weeks old) from Taconic Bioscience (Cambridge City, Indiana) were housed at the UCSF Preclinical Therapeutics Core vivarium (San Francisco, California). All animal studies were carried out in accordance with UCSF Institutional Animal Care and Use Committee. Tumor xenografts were established by subcutaneous injection with MX-1 tumor cells ($2x10^6$ cells in 100 µl of serum free medium mixed 1:1 with Matrigel) into the right flank of female NCr nude mice. When tumor xenografts reached 1000-1500 mm^3 in donor mice, they were resected, divided into even-size fragments (approximately 2.5 x 2.5 mm), embedded in Matrigel and re-implanted via subcutaneous trocar implantation in receiver mice (8). Tumors grown from implanted cells had an observed doubling time of ~11 days, whereas tumors grown from implanted tumor fragments doubled with the reported 5-6 days (9).

3. Dosing and tumor volume measurements: Solutions of PEG~SN-38 (**1A-1D**) prepared in isotonic acetate (pH 5), sterile filtered through a 0.2 µm syringe filter, and SN-38 content was determined according to the general procedure. When tumors reached ~100-200 mm^3 in size, dosing solutions were administered i.p. at ~14-16 mL/kg to deliver 4-120 µmol SN-38/kg as PEG~SN-38. Solutions of CPT-11 were prepared in isotonic acetate (pH 5) and sterile filtered through a 0.2 µm syringe filter before use.

Tumor volumes (caliper measurement: 0.5x(length x width^2)) and body weights were measured twice weekly.

4. Anti-tumor efficacy in MX-1 xenografts: The nomenclature used for describing disease in individual mice was as proposed by Houghton et al (10) and is summarized in **Table S2**.

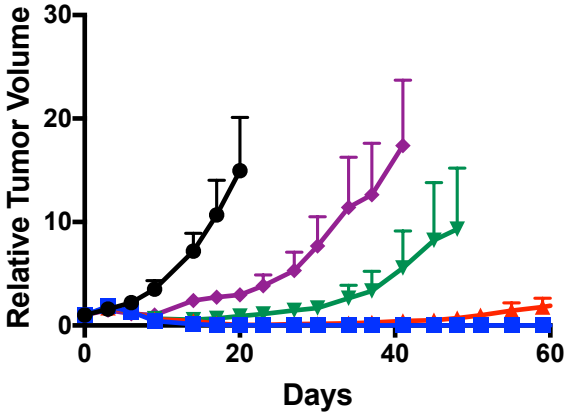

Figure S4. Additional dose response of MX-1 xenografts toward PLX038A (**1B**). Relative tumor volume versus time post dose: vehicle control (●) or single i.p. injections of 40 µmol/kg (■), 30 µmol/kg (▲), 20 µmol/kg (▼), and 10 µmol/kg (◆).

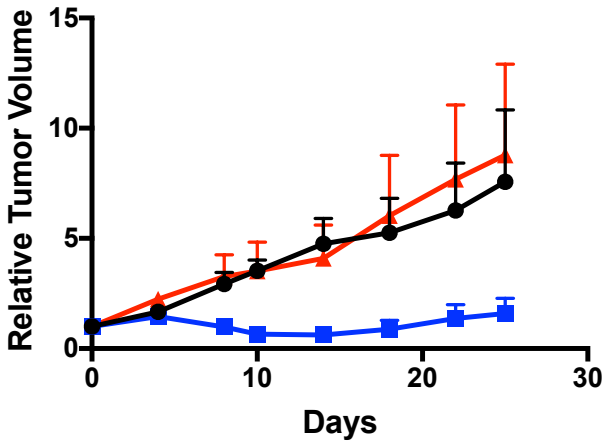

Figure S5. MX-1 response to equal doses (20 µmol/kg) of PLX038A (**1B**) or PLX038 (**1C**). Relative tumor volume versus time post dose: vehicle control (●) or single i.p. injections of 20 µmol/kg of PLX038A(**1B**, Mod=SO_2Me, ■), or PLX038 (**1C**, Mod = CN, ▲).

Table S2. Nomenclature describing disease in individual mice[a]

Name	Abb.	Description
Progressive disease 1	PD1	< 50% regression from initial volume during the study period and > 25% increase at the end; mouse had a TGD value ≤ 1.5
Progressive disease 2	PD2	PD1, and mouse had a TGD value > 1.5
Stable disease	SD	< 50% regression from initial volume during the study period and ≤ 25% increase at the end
Partial response	PR	tumor volume regression ≥50% for at least one time point but with measurable tumor (50 mm^3)
Complete response	CR	disappearance of measurable tumor mass (< 50 mm^3) for at least one time point
Maintained complete response	MCR	CR, and tumor volume was <50 mm^3 at the end of the study
Event		quadrupling of tumor volume from the initial tumor volume
Event-free survival	EFS	time to the first event, or to the end of the study for tumors that did not quadruple in volume
Tumor growth delay	TGD	time to event divided by the median time to event in the control group.

[a] PD was classified as PD1 or PD2 based on the tumor growth delay (TGD) values calculated as the number of days to event. For each mouse, TGD was calculated by dividing the time to event by the median time to event in the control group. For each individual mouse that had PD

and had an event in the treatment groups, a TGD value was calculated by dividing the time to event for that mouse by the median time to event in the control group. Median times to event were estimated based on the Kaplan-Meier event-free survival distribution.

Table S3. Anti-tumor effects of PLX038A and CPT-11 on individual tumor-bearing mice.

single dose µmol/kg	**PD1**	**PD2**	**SD**	**PR**	**CR**	**MCR**
PLX038A						
Small tumors						
4	3	1				
10		4				
13	1	3				
20		1	2		1	
30					3	1
40				3		5
120			1			8
Large tumors						
120					1	3
40					1	2
CPT-11						
Small tumors						
137	7	2				
PLX038						
Small tumors						
20	2	1	1			

References

1. Nabiev I, Fleury F, Kudelina I, Pommier Y, Charton F, Riou JF*, et al.* Spectroscopic and biochemical characterisation of self-aggregates formed by antitumor drugs of the camptothecin family: their possible role in the unique mode of drug action. Biochem Pharmacol **1998**;55:1163-74
2. Santi DV, Schneider EL, Ashley GW. Macromolecular prodrug that provides the irinotecan (CPT-11) active-metabolite SN-38 with ultralong half-life, low C(max), and low glucuronide formation. Journal of medicinal chemistry **2014**;57:2303-14
3. Schneider EL, Henise J, Reid R, Ashley GW, Santi DV. Hydrogel drug delivery system using self-cleaving covalent linkers for once-a-week administration of exenatide Bioconjugate chemistry **2016**;27:1210-15
4. Meier H, Petersen H. Synthese von 5-substituierten Cyclooctynen. Synthesis **1978**:596-8

5. Ranby M, Sundell IB, Nilsson TK. Blood collection in strong acidic citrate anticoagulant used in a study of dietary influence on basal tPA activity. Thromb Haemost **1989**;62:917-22
6. Li W, Zhang J, Tse FL. Strategies in quantitative LC-MS/MS analysis of unstable small molecules in biological matrices. Biomed Chromatogr **2011**;25:258-77
7. Tsujikawa K, Kuwayama K, Miyaguchi H, Kanamori T, Iwata YT, Inoue H. In vitro stability and metabolism of salvinorin A in rat plasma. Xenobiotica **2009**;39:391-8
8. Morton CL, Houghton PJ. Establishment of human tumor xenografts in immunodeficient mice. Nat Protoc **2007**;2:247-50
9. Ovejera AA, Houchens DP, Barker AD. Chemotherapy of human tumor xenografts in genetically athymic mice. Ann Clin Lab Sci **1978**;8:50-6
10. Houghton PJ, Morton CL, Tucker C, Payne D, Favours E, Cole C*, et al.* The pediatric preclinical testing program: description of models and early testing results. Pediatr Blood Cancer **2007**;49:928-40